J. Mater. Environ. Sci. 7 (8) (2016) 2869-2879
ISSN: 2028-2508
CODEN: JMESCN

Kinetics and thermodynamics study of methylene blue adsorption onto Aleppo pine cones

R. Elmoubarki[1], A. Moufti[1, 2], H. Tounsadi[1], F.Z. Mahjoubi[1], M. Farnane[1], A. Machrouhi[1], A. Elhalil[1], M. Abdennouri[1], A. Zouhri[3], N. Barka[1,*]

[1] *Laboratoire des Sciences des Matériaux, des Milieux et de la Modélisation (LS3M), FPK, Univ. Hassan 1, BP.145, 25000 Khouribga, Morocco.*

[2] *Regional Center for Careers in Education and Training. Settat. Morocco.*

[3]*Laboratoire Chimie Appliquée et Environnement, FST, Univ. Hassan 1, B.P. : 577, 26000 Settat, Morocco.*

Received 09 Mar 2016, Revised 05 Jul 2016, Accepted 07 Jul 2016
**Corresponding author. E-mail: barkanoureddine@yahoo.fr ; Tel.: +212 661 66 66 22; fax: +212 523 49 03 54*

Abstract

In this study, the adsorption of methylene blue (MB) onto *Aleppo Pine Cones* (APC) powder was investigated in batch mode. Series of experiments were then conducted to study the influence of some parameters on the adsorption capacity such as adsorbent mass, pH, contact time, initial concentration of the dye and temperature. The experimental results indicate that the adsorption yield increases with an increase in the adsorbent dosage and the initial concentration of dye in the solution. Results from the effect of pH indicate that MB is preferentially adsorbed in basic medium. The adsorption yield decreases with an increase in solution temperature. The overall results showed that the adsorption kinetics of the MB onto APC is well described by the pseudo-second order kinetic model. The adsorption isotherm was described satisfactorily by the mathematical model of Langmuir with a maximum monolayer adsorption capacity of 93.57 mg/g. Furthermore, the thermodynamic study revealed that the adsorption is spontaneous and exothermic.

Keywords: Aleppo pine cones, Adsorption, Dyes, Kinetics, Equilibrium, Thermodynamics.

1. Introduction

Synthetic dyes are among the most notorious organic contaminants that are discharged into the environment from textile, tanning, leather, paints, paper, food processing and pharmaceutical industries [1]. There are more than 100 000 types of dyes commercially available, with over 0.7 million tons of dyestuff produced annually. About 15% of these dyes are reported to get lost in the effluent [2]. The types of dyes used in the industries include cationic (basic dyes), anionic (direct, acid, and reactive dyes), and non-ionic dyes. Usually, even a very small amount of dye present in water is highly visible, even at very low concentrations. Most of the dyes are toxic and carcinogenic compounds; they are also recalcitrant and thus stable in the receiving environment, posing a serious threat to human and environmental health [3,4]. Accordingly, to protect humans and the receiving ecosystem from contamination, dyes must be eliminated from industrial effluents before discharging into the environment.

Several methods have been reported for the removal of dyes from industrial effluents and wastewaters, including, photodegradation [5], ozone [6], advanced oxidation processes [7], combined approach of electrochemical and biological [8], and adsorption [9]. Some of these techniques have been shown to be effective however they have some limitations such as excess amount of chemical usage, accumulation of concentrated sludge that has serious disposal problems and lack of effective color reduction.

The adsorption technique, which is based on the transfer of pollutants from the solution to the solid phase, is known as one of the efficient and general wastewater treatment method [10] and is becoming popular. The removal of the dyes in aqueous solutions by adsorption on different solid materials have recently been tested

such as stones olives [11], sunflower seed shells [12], Diplotaxis harra and Glebionis coronaria L. [13], nutshells [14], rice husks [15], corn shells [16], pistachio hull waste[17], fly ash [18], natural clays [19] and waste materials of Daucus carota [20]. The method is superior to other dyes removal techniques in terms of initial cost, simplicity of design, ease of operation, and non-toxicity of the utilized adsorbents compared to other conventional wastewater treatment methods [21,22].
In this work, we investigate the ability of Aleppo pine cones powder (APC) powder to adsorb organic dyes especially methylene blue. Results from the equilibrium and batch rate adsorption studies in aqueous solutions are given and adsorption capacities are obtained. The effects of contact time, initial dye concentration, adsorbent dosage, temperature and solution pH on the static adsorption of the dye were examined. The pseudo-first order and pseudo-second order kinetic models are used to correlate the adsorption kinetics data. The kinetics as well as the diffusion parameters was evaluated. Thermodynamic studies have also been performed to understand the processes.

2. Materials and methods

2.1. Preparation and characterization of the adsorbent

2.1.1. Materials

All the chemicals were reagent grade and were used without further treatment. Methylene blue (MB) was purchased from Sigma–Aldrich (Germany). NaOH was purchased from Merck (Germany), and HNO_3 from Scharlau (Spain). All solutions were prepared using deionizer water.

2.1.2. Preparation of the adsorbent (APC)

The *Aleppo Pine Cones (APC)* were collected from the region of Khouribga in Morocco. They were repeatedly washed with distilled water to remove dirt particles and then were air-dried. The dried cones were then cut into small pieces and powdered to particles of small sizes (φ<90µm, 90µm<φ<120µm and 120µm <φ<180µm) using a domestic mixer (APC).

2.2. Characterization

FTIR spectra were collected on a Nicolet Avatar 330 Fourier transform IR spectrophotometer. Samples were mixed with KBr at a mass ratio of 1:100 and finely powdered to prepare pellets. The spectra were recorded with 2 cm^{-1} resolution in the range of 4000–400 cm^{-1}. The elemental chemical analysis was carried out using a CHNOS Thermo Scientific Flash 2000 EA 1112 analyzer. The surface groups present on biosorbent were determined by Boehm titration; the acidic sites are determined by mixing small quantities (0.1g) of biosorbent with 10 mL of different bases (0.1 M NaOH, 0.1 M $NaHCO_3$, or 0.05 M Na_2CO_3) in 25mL beakers. Moreover, these beakers are sealed and shaken for 24 h. The solutions are then filtered and titrated with 0.05 M H_2SO_4. Similarly, the basic sites are determined by mixing 0.1 g of biosorbent with 10 mL of 0.1M HCl solution. The obtained solutions are titrated with 0.1M NaOH [23]. The point of zero charge (pH_{PZC}) was determined by the pH drift method according to the method proposed by Noh and Schwarz [24]. The pH of NaCl aqueous solution (50 ml at 0.01 mol/L) was adjusted to successive initial values in the range of 2 and 12 by addition of HNO_3 (0.1N) and/or NaOH (0.1N). More there, 0.05 g of each sorbent was added in solution and stirred for 6h. The final pH was measured and plotted versus the initial pH, the pH_{PZC} was determined by the value of which pH final= pH initial.

2.3. Adsorption experiments

The adsorption tests were carried out in a discontinuous reactor at room temperature in 100 ml flask containing the adsorbent material and the dye solution. The effect of the adsorbent dosage (R=m/V) where m is the adsorbent mass and V is the volume of dye solution), the initial pH and the initial concentration of the dye on adsorption (C_0) were studied separately.
The mixture was constantly stirred for a fixed time and then the equilibrium concentration (Ce) was determined by a UV–visible spectrophotometer (TOMOS V-1100 UV/Vis Spectrophotometer).

The amount of dye adsorbed per unit mass of adsorbent, or adsorption capacity, was calculated as:

$$q_{t,e} = \frac{(C_0 - C_{t,e})V}{m} \qquad (1)$$

where $q_{t,e}$ was the amount of dye adsorbed per gram of adsorbents (mg/g) at time and at equilibrium, C_0 and $C_{t,e}$ are the initial, at time and equilibrium concentrations (mg/L) of MB in solution, V is the volume of the solution (L), and m was the weight of the adsorbent (g).

3. Results and discussion

3.1. Characterization of the adsorbent

The biosorption capacity of Aleppo pine cones depends on physical as well as chemical reactivity of surface functional groups. This reactivity creates an imbalance between forces at the surface when compared to those within the body, thus leading to molecular biosorption by the Van Der Waals forces. Knowledge on surface functional groups would give insight to the biosorption capability of APC. The spectra of APC and MB loaded APC were shown in Fig.1. The main peak at 3761 and 3416 cm^{-1} in the spectra of APC was due to the presence of bounded hydroxyl (-OH) or amine (-NH) groups. The peak at 2925 cm^{-1} is attributed to the symmetric and asymmetric C-H stretching vibration of aliphatic acids [25]. The peak observed at 1741 cm^{-1} is the stretching vibration of bond due to nonionic carboxyl groups (-COOH, -$COOCH_3$) and may be assigned to carboxylic acids or their esters [25]. The bands at 1246 cm^{-1} indicate the C-O stretching in ether or alcohol and methoxy group, respectively. The bands 1649 cm^{-1} indicate functional group region of C=O, C-O, and O-H groups that exist as functional groups of APC. The peak at 1519 cm^{-1} is assigned to a conjugated hydrogen bonded carbonyl group. The peak at 1460 cm^{-1} indicates the presence of carboxyl groups (-COOH). The peaks at 1325 and 1378 cm^{-1} indicate the presence of C-H aliphatic bending. The peaks at 1048 and 604 cm^{-1} indicate the presence of alkyl halide (C-F, C-Cl). In comparing the two spectra of MB and APC alone with that of APC+MB, it is observed the disappearance of the following bands 1519 cm^{-1}, 13278 cm^{-1}, 1325 cm^{-1} and 1246 cm^{-1}. From Table 1, we see the existence of carbon and oxygen in large quantities (C = 45.58 % and O = 44.4%), hydrogen in small quantities (6%) for nitrogen and sulfur are virtually missing. From the results obtained by the Boehm titration, it can be observed that the amount of acidic groups was significantly higher than total amount of basic groups. These results suggest that APC has an acidic character; these findings are quite consistent with the FTIR spectrum.

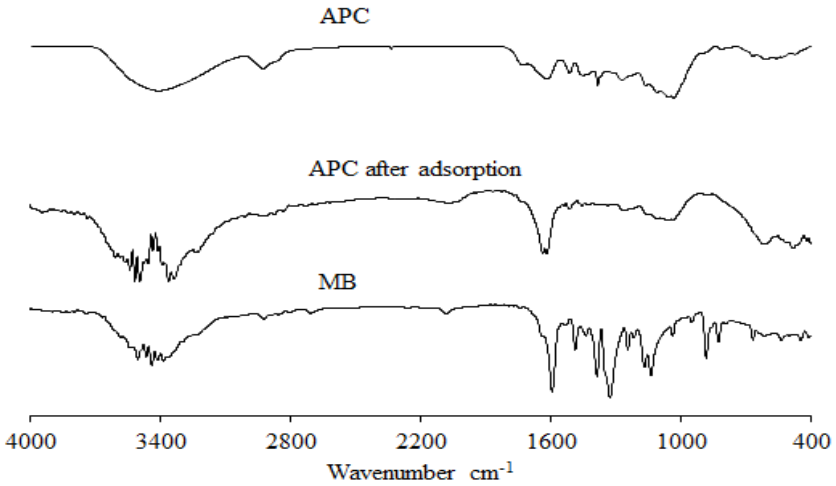

Fig.1: FT-IR spectra of APC, MB and MB loaded APC.

3.2. Effect of pH

The pH is an important factor in any adsorption study, because it can influence at the same time the adsorbent, adsorbate and the adsorption mechanism. In this paper, we studied the adsorption efficacy of MB by varying the pH from 2 to 10. Under these pH conditions, a mass of 50 mg of the adsorbent was stirred in 100 ml of the colored solution. The results obtained from these tests, are presented in Fig.2. From the figure, it is evident that

increasing solution pH serves to the increase of the adsorption capacity, with a significant enhancement from 15% to 80%; this can be attributed to the protonation of MB in the acidic medium, and presence of excess H^+ ions, competing with dye cations for the adsorption sites. However, at higher solution pH, the formation of electric double layer changes its polarity and consequently the dye uptake increases, this result agrees with the finding of other researchers [26].

Table 1: Functional groups and elemental chemical analysis of APC.

Functional groups (mmol/g)		Elemental analysis (%,weight)	
Carboxylic	0.250	C	45.58
Phenolic	0.200	O	44.40
Lactonic	0.170	H	6.07
Total acid groups	0.620	N	0.47
Total basic groups	0.458		
pH_{PZC}	5.53		

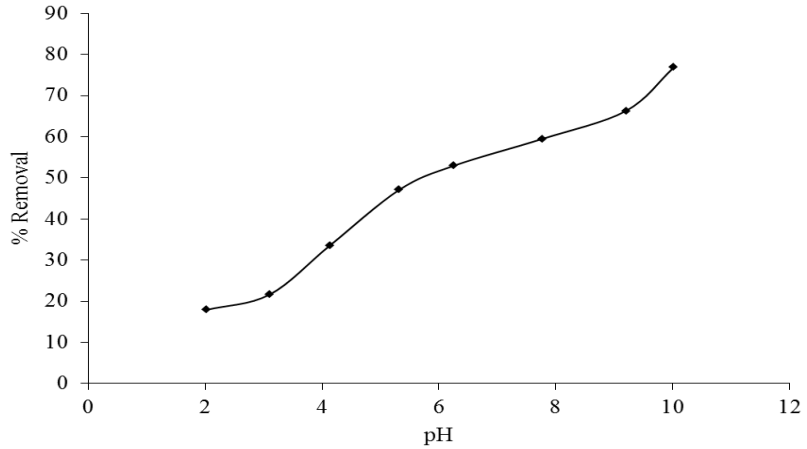

Fig.2: Effect of pH on equilibrium uptake of MB. Conditions: agitation time = 2 h; C_0=100mg/L; V = 100mL; speed of agitation = 360 rpm; R = 0.5g/L.

3.3. Adsorption kinetics

The effect of APC size on the amount of MB adsorbed was obtained by adding a mass of APC at different size (φ<90µm, 90µm<φ<125µm, 125µm<φ<180µm) into glass erlenmeyer flasks containing a definite volume (100mL in each case) of fixed initial concentration (100mg/L) of solution without changing pH (5.35) and at room temperature. The results are illustrated in Fig.3 in terms of MB removal as a function of contact time. The figure makes two important points; first, for all levels of APC size, the removal percentage improved with the increase of contact time, with the highest rate at the initial contact times. This can be attributed to free adsorption sites available at the initial phases of the test [27], as well as to a small particle size rate at initial contact times where a higher concentration of MB is available to be adsorbed, thus, the rate of adsorption was greater. The second point, at a contact time (120min), the removal percentage of MB stabilize for the three used sizes [27].

3.4. Kinetic modeling of the adsorption

Kinetic modeling of the adsorption process provides a prediction of adsorption rates, and allows the determination of fitting rate expressions characteristic for possible reaction mechanisms. The most frequently used models are the pseudo-first-order and the pseudo-second-order. The models were analyzed based on the regression coefficient, (r^2), and the amount of dyes adsorbed at equilibrium. The pseudo-first-order rate expression of Lagergren based on solid capacity is generally expressed as follows [28]:

$$q = q_e(1 - e^{-k_1 t}) \quad (2)$$

where q_e and q (both in mg/g) are respectively the amounts of dye adsorbed at equilibrium and at any time't', and k_1 (1/min) is the rate constant of adsorption.

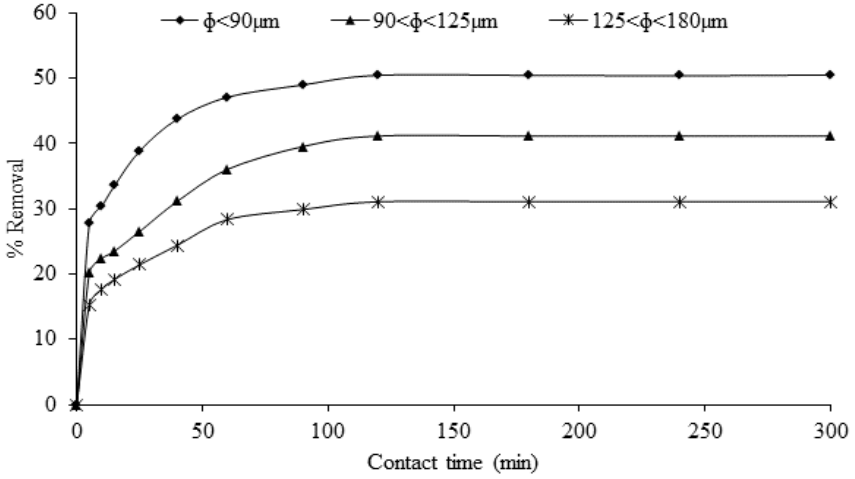

Fig.3: Effect of particle size on kinetics of MB adsorption. Conditions: agitation time = 2 h; C_0=100mg/L; V = 100 mL; speed of agitation = 360 rpm; R = 0.5g/L.

The pseudo-second-order model proposed by Ho and Mckay [29] was used to explain the sorption kinetics. This model is based on the assumption that the adsorption follows second order chemisorption. The pseudo-second-order model can be expressed as:

$$q = \frac{k_2 q_e^2 t}{1 + k_2 q_e t} \quad (3)$$

The parameters of the two kinetic models, calculated by the software Origin, are summarized in Table 2. From these results it is seen that in the case of first order model, the amount adsorbed to balance experimentally determined is different from that calculated. For against, the amount adsorbed to balance, determined experimentally is closer to that calculated using the kinetic model of the pseudo second order. This model does apply in the case of systems adsorbent/adsorbate studied saw values r^2 obtained coefficients of determination which are very close to unity.

Table 2: Pseudo-first order and pseudo-second order kinetic parameters for MB adsorption.

		Pseudo-first-order			Pseudo-second-order		
	q_{exp} (mg/g)	q_e (mg/g)	k_1 (1/min)	r^2	q_e (mg/g)	k_2 (g/mg min)	r^2
φ <90µm	99.59	95.28	0.0988	0.937	101.62	0.0016	0.983
90< φ <125µm	81.10	77.22	0.0669	0.901	83.45	0.0012	0.960
125< φ <180µm	61.24	58.36	0.0778	0.920	62.87	0.0019	0.974

3.5. Intra-particle diffusion process

For the interpretation of experimental kinetics data, from a mechanistic viewpoint, prediction of the rate-limiting step is of important consideration. The adsorbate transport from the solution phase to the surface of the adsorbent particles occurs in several steps. The overall adsorption process may be controlled either by one or more steps, e.g. film or external diffusion, pore diffusion, surface diffusion and adsorption on the pore surface, or a combination of more than one step. The possibility of intra-particle diffusion was explored by using the Weber–Morris intra-particle diffusion model [30]:

$$q = k_{id} t^{0.5} + I \quad (4)$$

where k_{id} is the intra-particle diffusion rate constant (mg/g $min^{1/2}$) and I (mg/g) is a constant.

If the Weber–Morris plot of q versus $t^{0.5}$ satisfies a linear relationship with the experimental data, then the sorption process is found to be controlled by intra-particle diffusion only. However, if the data exhibit multi-linear plots, then two or more steps influence the sorption process. Fig.4 shows the traces of intra-particle diffusion model for the three adsorbent particle sizes used in this study (φ<90µm, 90<φ<125µm and 125<φ <180µm. The values of the constant outreach k_{id}, as well as those of r^2 are given in Table 3. From the figure, it is easy to see that the internal diffusion is a significant step in the process of adsorption of MB on the APC, particularly from the first 4 minutes up to 64 minutes and after we note a partial decrease or stabilization. This latency can be explained by the movement of the dye molecules in the pores of the adsorbent, before reaching the surface where they will arrange in layers. However, the chemical reaction surface, starting from the first minutes of contact time with the experimental points line the pseudo-second order with a very high regression coefficients (r^2) indicates that the most influential stage in dye adsorption remains the internal diffusion process, since it can be considered limiting step that controls the transfer rate of the dye at each time "*t"* [31].

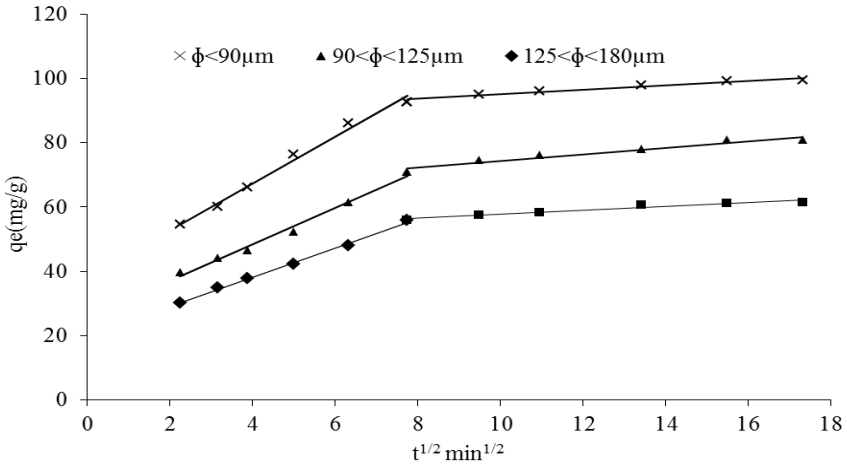

Fig.4: Application of the intra-particle diffusion model to the adsorption of MB on APC.

Table 3: Parameters of Intra-particle diffusion model.

	k_{id} (mg/g $min^{0.5}$)	*I* (mg/g)	r^2	k'_{id} (mg/g $min^{0.5}$)	*I'* (mg/g)	r^2
φ<90µm	7.288	38.283	0.989	0.697	88.225	0.949
90<φ<125µm	5.692	25.594	0.987	1.0208	64.258	0.948
125<φ<180µm	4.550	19.998	0.996	0.603	51.671	0.935

3.6. Effect of adsorbent dose

The result from the effect of APC dose on MB adsorption was performed in a range of 0.25 to 2g/L. Fig.5 makes two important points. First, for all levels of APC dose, the removal percentage improved with the increase of contact time, with the highest rate in the initial times. This can be attributed to free adsorption sites available at the initial phases of the process [27]. As well as to a higher mass transfer rate at initial contact times where a higher concentration of MB is available to be adsorbed. Thus, the rate of adsorption was greater. The second point in Fig.5 is the increase in MB removal with the increase of APC dose, resulting in a shorter treatment time. According to the figure around 15.36, 58.00 and 92% of 100mg/L MB was removed in the first minutes of contact time (40min). The removal efficiency reached a maximum of 40, 66 and 92% with doses of 0.5, 1 and 2g/L, respectively. The enhancement of MB removal as a function of APC dose is due to the presence of a greater surface for adsorption and thus more available sites [32] for MB molecules to be adsorbed, leading to the uptake of more molecules. It is readily understood that the number of available adsorption sites increases

by increasing the adsorbent dose. Therefore, results in an increase in the amount of adsorbed dye [33]. The stability in adsorption density with an increase in the adsorbent dose is mainly because of adsorption sites remain unsaturated during the adsorption reaction whereas the number of sites available for adsorption site increases by increasing the adsorbent dose [34,35].

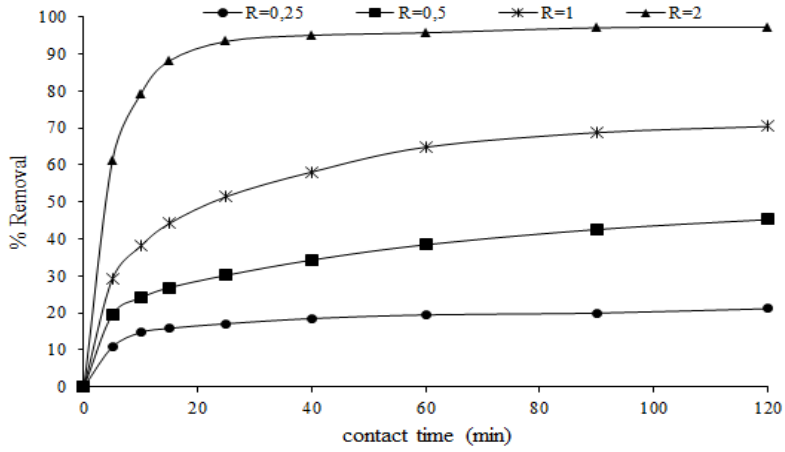

Fig.5: Effect of adsorbent dose on the adsorption of MB. Conditions: agitation time = 2 h; C_0 = 100mg/L; V = 100ml; agitation speed = 360 rpm.

3.7. Isotherm of MB adsorption onto APC

The analysis of equilibrium adsorption isotherm provides information about the surface properties of adsorbent, which help in the design of adsorption systems. Adsorption equilibrium is a dynamic concept achieved as the rate of dye adsorption is equal to the rate of desorption [36]. Several models including Langmuir, Freundlich and Dubinin–Radushkevich were used to analyze the adsorption isotherm (Fig.6). The Langmuir adsorption model is established on the following hypotheses: (1) uniformly energetic adsorption sites, (2) monolayer coverage, and (3) no lateral interaction between adsorbed molecules. Graphically, a plateau characterizes the Langmuir isotherm. Therefore, at equilibrium, a saturation point is reached where no further adsorption can occur. A basic assumption is that sorption takes place at specific homogeneous sites within the adsorbent. Once a dye molecule occupies a site, no further adsorption can take place at that site. The non-linearized form of Langmuir isotherm model can be described as the following equation [37]:

$$q_e = \frac{q_m K_L C_e}{1+K_L C_e} \qquad (5)$$

where K_L (L/mg) is the Langmuir adsorption constant related to the energy of adsorption. q_m and q_e (mg/g) are the maximum and equilibrium adsorption capacity, respectively.

The Freundlich isotherm endorses the heterogeneity of the surface and assumes that the adsorption occurs at sites with different energy of adsorption. The energy of adsorption varies as a function of surface coverage. The non-linearized form of Freundlich isotherm model is given as the following equation [30]:

$$q_e = K_F C_e^{1/n} \qquad (6)$$

where K_F (L/mg) is the Freundlich constant and 1/n is the heterogeneity factor.

The Dubinin–Radushkevich isotherm model is an empirical model applied to determine the characteristic porosity and the apparent free energy of adsorption. The model does not assume a homogenous surface or constant sorption potential as other models. It can be noted that the (D–R) isotherm is more general that the Langmuir fit. The D–R isotherm has been written by the following equations [38]:

$$q_e = q_m \exp\left(-B\varepsilon^2\right) \qquad (7)$$

$$\varepsilon^2 = RT \ln\left(1+\frac{1}{Ce}\right) \qquad (8)$$

where B is a constant related to the adsorption energy, q_m is the theoretical saturation capacity, ε is the Polanyi potential. The corresponding parameters of Langmuir, Freundlich and Dubinin–Radushkevich are given in Table 4. From the table, the r^2 of the Langmuir isotherm model (r^2=0.998) was higher than those of the other models (r^2=0.966 for Freundlich and r^2=0.925 for Dubinin–Radushkevich). This result indicates that the experimental equilibrium data was better explained by the Langmuir equation. This finding supports the assumption that the MB is adsorbed as a homogeneous monolayer onto APC particles sites and has a free-energy change for all adsorption sites [39].

The maximum monolayer adsorption capacity was 97.03 mg/g. This capacity was compared to the previous records of various low-cost biosorption as summarized in Table 5. It can be observed that experimental data of the present study was found to be higher than those of most corresponding biosorbents in the literature.

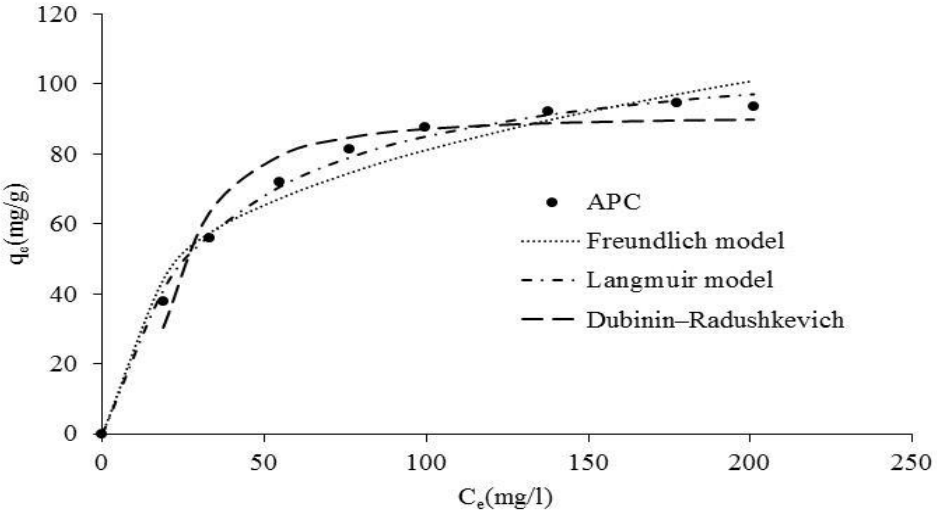

Fig.6: Adsorption isotherm of MB onto APC (Conditions: agitation time = 2h; C_e (20-200) mg/L; V = 100ml; speed of agitation = 360 rpm. R = 0.5g/L).

Table 4: Langmuir, Freundlich and Dubinin–Radushkevich parameters

Langmuir				Freundlich			Dubinin–Radushkevich		
q_{exp}(mg/g)	q_m(mg/g)	K_L	r^2	K_F	n	r^2	q_m(mg/g)	B (mol/J)	r^2
90.58	97.03	0.034	0.998	19.253	3.204	0.966	90.674	0.164	0.925

Table 5: Comparison of maximum biosorption capacity of *APC* for MB with corresponding biosorbents.

Biosorbent	q_m(mg/g)	References
Rice husk	40.59	[40]
Cotton waste	277.77	[41]
Papaya seeds	555.55	[42]
Coconut husk	99.00	[43]
Coffee husks	90.10	[44]
Teak wood bark	84.00	[45]
Raw date pits	80.30	[46]
Banana peel	20.80	[47]
Cereal chaff	20.30	[48]
Aleppo pine cones	97.03	This study

3.8. Effect of temperature and thermodynamics of MB adsorption onto APC

The effect of solution temperature on equilibrium adsorption of MB by APC was studied in the temperature range of 20, 30, 40 and 50°C. Fig.7 depicts the effect of temperature on the removal efficiency. Based on data plotted in figure, the increase of solution temperature from 20 to 50°C resulted in a large decrease of the equilibrium removal percentage of MB from 45 to 35% under the selected experimental conditions. It was observed that we have a decrease in discoloration with increasing temperature. The increase of temperature, disadvantage the progress of the adsorption phenomenon. It can be therefore inferred from these finding that MB adsorption onto APC is an exothermic phenomenon [49].

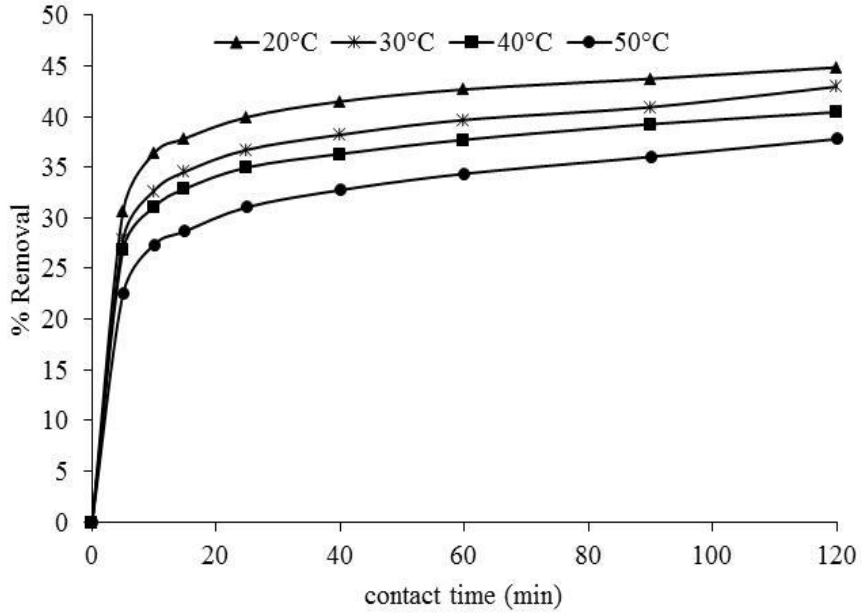

Fig.7: Effect of temperature on the adsorption of MB onto APC (Conditions: agitation time = 2 h; C_0=100 mg/L; V = 100mL; speed of agitation = 360 rpm. R = 0.5g/L)

The experimental data obtained for MB, adsorption on APC adsorbent at different temperatures were used for calculation of thermodynamic parameters, such as Gibbs free energy (ΔG°), enthalpy variation (ΔH°) and entropy variation (ΔS°). For such equilibrium reactions, K_D, the distribution constant, can be expressed as:

$$K_D = \frac{q_e}{C_e} \quad (9)$$

The Gibbs free energy is:

$$\Delta G° = -RT \ln (K_D) \quad (10)$$

where R is the universal gas constant (8.314 J mol/K) and T is solution temperature in K. The enthalpy (ΔH°) and entropy (ΔS°) of adsorption were estimated from the slope and intercept of the plot of $\ln K_D$ versus 1/T yields, respectively.

$$\mathrm{Ln}\, K_D = -\frac{\Delta G°}{RT} = -\frac{\Delta H°}{RT} + \frac{\Delta S°}{R} \quad (11)$$

As seen in Table 6, the value of ΔG°, ΔH°, and ΔS° for all tested temperatures was calculated to be negative, which suggests that the adsorption of MB onto APC is spontaneous and exothermic and indicates that APC has a high affinity for the adsorption of MB from solution under experimental conditions [50]. Values of Δ*G* between −20 and 0 kJ/mol indicate a physical adsorption process [51].

Table 6: Thermodynamic parameters calculated for the adsorption of MB by the APC.

	MB				
T (°C)	q_e(mg/g)	K_D	ΔG° (J/mol)	ΔH° (kJ/mol)	ΔS° (J/K.mol)
20	88.41	1.627	-1.186	-7.23	-20.55
30	84.69	1.507	-1.033		
40	79.72	1.358	-0.797		
50	74.48	1.239	-0.576		

Conclusion

This study shows that Aleppo pine cones powder (APC) can efficiently remove dyes from aqueous solutions, especially methylene blue (MB). The adsorption was dependent on the pH of the aqueous solution with a high uptake of the dye at high pH. The adsorption was rapid and could be considered to fit pseudo-second order kinetics model with good correlation. The equilibrium uptake was increased with increasing the initial concentration of dye in solution and the APC dose. Equilibrium data were best described by the Langmuir isotherm model and the adsorption process was of physical nature. The rise in temperature increases the adsorbed amount of methylene blue dye. These results suggest that the adsorption of cationic dye (MB) by the APC be spontaneous and exothermic. Results of present study have been satisfactory and they indicate the potential of Aleppo pine cone for removal of MB from the aqueous solution because it is a low-cost and eco-friendly adsorbent. Finally, the use of Aleppo pine cone shows greater potential for the removal of textile dyes.

Acknowledgement-The authors acknowledge the University Hassan 1er for technical support during this study.

References

1. Extremera R., Pavlovic I., Pérez M. R., Barriga C., *Chem. Eng. J.* 213 (2012) 392.
2. Crini G., *Bioresour. Technol*, 97 (2006) 1061.
3. Li S., *Bioresour. Technol.* 101 (2010) 2197.
4. Bao N., Li Y., Wei Z., Yin G., Niu J., *J. Phys. Chem. C* 115 (2011) 5708.
5. Abaamrane A., Qourzal S., Barka N., Mançour-Billah S., Assabbane A. Ait-Ichou Y., *Orient. J. Chem.* 28(3) (2012) 1091.
6. Panda K. K. Mathews A. P., *Chem. Eng. J*, 255 (2014) 553.
7. Karci A., *Chemosphere* 99 (2014) 1.
8. Pramila M., Manikandan S., Anju K. S., Murali Kannan M., Hong S., Maruthamuthu S., Subramanian K., *Sep. Purif. Technol*, 132 (2014) 719.
9. Barka N., Assabbane A., Aît Ichou Y. Nounah A., *Journal of Applied Sciences*, 6(3) (2006) 692.
10. Ghaedi M., Sadeghian B., Pebdani A. A., Sahraei R., Daneshfar A., Duran C., *Chem. Eng. J*, 187 (2012) 133.
11. Hemsas S., Lounici H., Belkebi Z., Benrachedi K. 4 (2014) 414.
12. Thinakaran N., Baskaralingam P., Pulikesi M., Panneerselvam P., Sivanesan S., *J. Hazard. Mater*, 151 (2008) 316.
13. Tounsadi H., Khalidi A., Abdennouri M., Barka N., *Desal. Water Treat*. 57(35) (2016) 16633.
14. Bulut Y. Aydın H., *Desalination* 194 (2006) 259.
15. Malik P. K., *Dye. Pigment*, 56 (2003) 239.
16. Maghri B. I., Amegrissi F., Elkouali M., Kenz A., *Glob. J. Sci. Front. Res. Chem*, 12 (2012) 1.
17. Moussavi G., Khosravi R., *Chem. Eng. Res. Des.* 89 (2011) 2182.
18. Barka N., Ouzaouit K., Abdennouri M., El Makhfouk M., *J. Taiwan Inst. Chem. Eng*. 44 (2013) 52.
19. Elmoubarki R., Mahjoubi F. Z., Tounsadi H., Moustadraf J., Abdennouri M., Zouhri A., El Albani A., Barka N., *Water Resour. Ind*, 9 (2015) 16.
20. Kushwaha A. K., Gupta N., Chattopadhyaya M.C., *J. Saudi Chem. Soc*.18 (2014) 200.
21. Chiou M. S. Chuang G. S., *Chemosphere* 62 (2006) 731.
22. Barka N., Abdennouri M., El Makhfouk M., *J. Taiwan Inst. Chem. Eng.* 42 (2011) 320.
23. Kalijadis A., Vukcevic M., Jovanovic Z., Lausevic Z., Lausevic M., *J. Serbian Chem. Soc*, 76 (2011) 757.

24. Ghasemi M., Zeinaly Khosroshahy M., Bavand Abbasabadi A., Ghasemi N., Javadian H., Fattahi M., *Powder Technol*, 274, (2015) 362.
25. Li F.T., Yang H., Zhao Y., Xu R., *Chinese Chem. Lett*, 18 (2007) 325.
26. Foo K. Y., Hameed B. H., *Biomass and Bioenergy* 35 (2011) 3257.
27. Kavitha D., Namasivayam C., *Bioresour. Technol*, 98 (2007) 14.
28. Lagergren S., *Sven K..Vetenskapsakademiens Handl*, 24 (1898) 1.
29. Ho Y. S., Mckay G., *Can. J. Chem. Eng*, 76 (1998) 822.
30. Weber W. J., Morris J. C., *J. Sanit. Eng. Div. Am Soc Civ Engrs* 89 (1963) 31.
31. Belaid K. D., Kacha S., *Rev. des Sci. l'eau* 24 (2011) 131.
32. Hameed B. H., *J. Hazard. Mater*, 162 (2009) 344.
33. Shahul Hameed K., Muthirulan P., Meenakshi Sundaram M., *Arab. J. Chem.* 2013.
34. Malik R., Ramteke D. S., Wate S. R., *Waste Manag*, 27 (2007) 1129.
35. Yener J., Kopac T., Dogu G., Dogu T., *J. Colloid Interface Sci.* 294 (2006) 255.
36. Fu J., Chen Z., Wang M., Liu S., Zhang J., Zhang J., Han R., Xu Q., *Chem. Eng. J.* 259 (2015) 53.
37. Chen L., Bai B., *Ind. Eng. Chem. Res*, 52 (2013) 15568.
38. Dubinin M.M., Radushkevich L.V., *Proc. Acad. Sci. USSR Phys. Chem. Soc* 55 (1947) 331.
39. Crittenden J. C., Trussell R. R., Hand D. W., Howe K. J., Tchobanoglous G., Water Treatment: Principals and Design, 2nd ed. MWH, John Wiley and Sons, Inc, 2005.
40. Vadivelan V., Kumar K.V., *J. Colloid. Interface Sci*. 286 (2005) 90.
41. McKay G., Porter J.F., Ramprasad G., *Water Air Soil Pollut*. 114 (1999) 423.
42. Hameed B.H., *J. Hazard. Mater*. 162 (2009) 939.
43. Low K.S., Lee C.K., *Pertanika* 13 (1990) 221.
44. Oliveira L.S., Franca A.S., Alves T.M., Rocha S.D.F., *J. Hazard. Mater*. 155 (2008) 507.
45. McKay G., Ramprasad G., Pratapamowli P., *Water Air Soil Pollut*. 29 (1986) 273.
46. Banat F., Al-Asheh S., Al-Makhadmeh L., *Process Biochem*. 39 (2003) 193.
47. Annadurai G., Juang R., Lee D., *J. Hazard. Mater*. 92 (2002) 263.
48. Han R., Wang Y., Han P., Shi J., Yang J., Lu Y., *J. Hazard. Mater*. 37 (2006) 550.
49. Fu J., Chen Z., Wang M., Liu S., Zhang J., Zhang J., Han R., Xu Q., *Chem. Eng. J.*, 259 (2015) 53.
50. Crini G., *Dye. Pigment.* 77 (2008) 415.
51. Almeida C.A.P., Debacher N.A., Downs A.J., Cottet L., Mello C.A.D., *J. Colloid Interface Sci*, 332 (2009) 46.

(2016); http://www.jmaterenvironsci.com/